SYNTHESIS, CHARACTERIZATION AND STUDY OF THE ANTIBACTERIAL AND ANTIOXIDANT ACTIVITY OF Cu(II) and Cd(II) COMPLEXES USING MANNICH BASES AND PHOSPHINATES (dppe, dppp) AS LIGANDS

A.H. Hamad Al_Mofrajy, A.S. Shihab

College of Education for Pure Science, Department of Chemistry, Tikrit University, Tikrit, Iraq
e-mail: AH230028pep@st.tu.edu.iq

Received 09.07.2025
Accepted 18.09.2025

Abstract: *Drug-resistant bacteria, especially multidrug-resistant strains, chronic infections, and emerging pathogens, continue to evolve and spread widely. This development places a significant burden on the global healthcare system, and there is an urgent need to develop new and highly effective antibacterial drugs. In this study, several Mannich bases derived from 2-aminothiazole and diphenylbenzene with benzaldehyde substitutes were prepared. The prepared Mannich bases were used as ligands to prepare copper and cadmium complexes. Finally, the prepared complexes were reacted with phosphines (dppe, dppp) to prepare various complexes in an attempt to synthesize more potent compounds. Physical characteristics such as melting point and color were used to validate the structures of the free compounds. The compounds were also characterized spectroscopically using infrared spectroscopy, proton and phosphorus nuclear magnetic resonance (NMR), quantitative elemental analysis (C.H.N.), and magnetic susceptibility studies of the formed complexes. Some compounds showed good activity against Gram-negative and Gram-positive bacteria, with compound (A_{34}) having the largest share, as it showed excellent activity, reaching an inhibition rate of (34 mm) against Staphylococcus aureus and an inhibition rate of (24 mm) against* ***Escherichia coli****. In an additional study, the antioxidant activity of the compounds prepared outside the body was studied, where the compound (A_{34}) showed excellent activity, reaching (58.75%) and this is a good indicator of the effectiveness of the compounds as antioxidants.*

Keywords: *Complex, Mannich bases antioxidant, Biological activity, Cu(II), Cd(II).*
DOI: 10.65382/2221-8688-2026-4-525-539

1. Introduction

Organic compounds containing nitrogen, carbonyl, and oxygen atoms—as well as their metal complexes—play essential roles across numerous industrial and scientific fields. Their applications span industrial synthesis [1], agriculture [2], environmental chemistry [3], catalysis, analytical chemistry, and biomedical sciences [4–6]. Among the foundational transformations in organic chemistry, the Mannich reaction stands out as a highly influential synthetic pathway that has profoundly shaped the development of both organic chemistry and biochemistry. The Mannich reaction is considered one of the fundamental carbon–carbon and carbon–nitrogen bond-forming methods and is widely used in the preparation of pharmaceuticals, including antibacterial and antiprotozoal agents [7], as well as a variety of natural products and biologically active molecules [8, 9]. It also serves as a key route for generating valuable intermediates required in the pharmaceutical industry. Moreover, Mannich-type ligands—characterized by nitrogen, carbonyl, and oxygen donor atoms—have gained significant attention in coordination and inorganic chemistry. These ligands function effectively as chelating agents [10], forming stable metal complexes with diverse structural and functional properties. In coordination chemistry, such complexes are particularly important due to their biomimetic behavior and their potential to model biological metal–ligand interactions [11]. Antianginal, anticancer, antituberculosis, anthelmintic, hypolipidemic, and flavoring activities have all been demonstrated by Mannich metal complexes [11, 12]. Additionally, in the treatment of water and wastewater, Mannich compounds are

regarded as heavy metal scavengers [13]. Mannich bases are crucial drug carriers for the synthesis of numerous high-value medicinal medicines because they include aminoalkyl chains. Along with a variety of biocatalytic, antiseptic, and detergent actions, they also have anti-inflammatory, anticancer, antibacterial, antifungal, anticonvulsant, and antiviral qualities [14, 15]. Mannich bases can be synthesized either from purely organic reagents or through coordination with inorganic metal ions [15, 16]. It has also been shown that a variety of metal complexes are capable of catalyzing Mannich reactions [17].

The aim of this study is to synthesize a series of copper and cadmium complexes by reacting metal salts with Mannich bases to obtain Mannich-type coordination compounds, followed by their subsequent reaction with phosphines to form phosphine-containing complexes. The biological activities of these complexes, including their antibacterial properties and antioxidant potential, will then be evaluated.

2. Experimental Part

2.1. Material: All of the chemicals used in this study were purchased from BDH, Fluka, and Aldrich without any futher purification.

2.2. Preparation of Mannich base derivatives (A_{10}-A_{14}) [18, 19]. 2-Aminothiazole (0.003 mol, 1.6 g) was dissolved in approximately 15 mL of absolute ethanol and stirred at 50–60 °C. A solution of diphenylamine (0.003 mol, 1.4 g) in 15 mL of absolute ethanol was then added, and the mixture was stirred for 30 minutes. Subsequently, 0.003 mol of the corresponding substituted benzaldehyde, dissolved in a minimal amount of ethanol, was added dropwise to the reaction mixture. The reaction was allowed to proceed with continuous stirring for 4–6 hours. Thin-layer chromatography (TLC) was used to monitor and confirm completion of the reaction. After completion, the mixture was cooled slowly to room temperature, and the precipitate was filtered, collected, and dried to a constant weight. The crude product was then purified by recrystallization from ethanol. The physical properties are shown in Table 1.

Table 1. Some physical properties and percentage of Mannich compounds (A_{10}-A_{14})

Comp No.	R	Molecular Formula	Color	M.P. (^{0}C)	Yield (%)
A_{10}	4-Br	$C_{22}H_{18}BrN_3S$	Yellow	138-140	75
A_{11}	4-Cl	$C_{22}H_{18}ClN_3S$	Yellow	132-135	74
A_{12}	2,3-Cl	$C_{22}H_{17}Cl_2N_3S$	Light Yellow	130-133	78
A_{13}	4-NO_2	$C_{22}H_{18}N_4O_2S$	Brown	141-144	73
A_{14}	4-OH	$C_{22}H_{19}N_3OS$	Dark Yellow	112-115	71

2.3. Preparation of Mannich base complex (A_{32}-A_{35}) [20, 21]. A mixture of the Mannich compounds [A_{10}, A_{11}] (0.002 mol) and the metal nitrate $M(NO_3)_2 \cdot 6H_2O$ (0.001 mol) was thoroughly ground in a ceramic mortar for approximately 1.5 hours until a noticeable color change occurred, indicating complex formation. The resulting product was then washed with cold water to remove unreacted materials and subsequently recrystallized from ethanol to obtain the purified complex. Table 2 shows the physical properties of the prepared complexes [A_{32}-A_{35}].

Table 2. Some physical properties of the prepared complexes [A_{32}-A_{35}]

Comp No.	R	Complexes	Color	M.P (^{0}C)	Yield (%)
A_{32}	Br	$[Cu(A_{10})_2(H_2O)_2]$	Brown	176-178	60
A_{33}	Cl	$[Cu(A_{11})_2(H_2O)_2]$	Yellow	181-184	58
A_{34}	Br	$[Cd(A_{10})_2(H_2O)_2]$	Light Yellow	201-203	62

A_{35}	Cl	$[Cd(A_{11})_2(H_2O)_2]$	Brown	139-142	55

2.4. Preparation of phosphine complexes of Mannich bases (A_{36}-A_{43}) [22, 23]. A hot solution of phosphines (dppe, dppp) (0.001 mol), dissolved in a minimal volume of chloroform, was added to the previously prepared complexes [A_{32}–A_{35}] (0.001 mol), also dissolved in a small amount of chloroform. The reaction mixture was heated in a water bath with continuous stirring for 3–4 hours. After completion, the solution was concentrated, allowed to cool, and filtered. The resulting precipitate was collected and washed with diethyl ether. Table 3 shows the physical properties of the complexes [A_{36}-A_{43}].

Table 3. Some physical properties of the complexes [A_{36}-A_{43}]

Comp No.	R	Complexes	Color	M.P(^{0}C)	Yield (%)
A_{36}	Br	$[Cu(A_{10})_2(dppe)]$	Light yellow	168-170	59
A_{37}	Br	$[Cu(A_{10})_2(dppp)]$	Orange	155-158	63
A_{38}	Cl	$[Cu(A_{11})_2(dppe)]$	Green	132-135	62
A_{39}	Cl	$[Cu(A_{11})_2(dppp)]$	Light Green	141-143	67
A_{40}	Br	$[Cd(A_{10})_2(dppe)]$	yellow	145-148	61
A_{41}	Br	$[Cd(A_{10})_2(dppp)]$	Dark yellow	173-176	62
A_{42}	Cl	$[Cd(A_{11})_2(dppe)]$	Light Brown	167-170	57
A_{43}	Cl	$[Cd(A_{11})_2(dppp)]$	Brown	193-196	56

2.5. Evaluation of bacterial bioactivity. Two bacterial strains—***Staphylococcus aureus*** (Gram-positive) and ***Escherichia coli*** (Gram-negative)—were obtained from the central laboratory at Tikrit University. To prepare Mueller-Hinton agar, 20 grams of each strain were dissolved in 500 milliliters of distilled water and stirred thoroughly until completely dissolved. The mixture was then sterilized in an autoclave at 1.5 bar pressure and 120°C for 14 minutes. After cooling, the medium was poured into Petri dishes and left to dry at 25°C [24, 25]. Test compound solutions were prepared in dimethyl sulfoxide (DMSO) at concentrations of 25%, 50%, and 100% (mg/ml). Once the culture medium solidified, the bacterial samples were spread evenly in three directions across the surface of the Petri dishes to ensure uniform distribution. Three wells were then created in each dish using a cork borer with a 6 mm diameter, and the prepared solutions were added to these wells [26, 27]. The plates were incubated at 37°C for 24 hours in a controlled environment. After incubation, the zones of inhibition were measured in millimeters using a ruler. ***Amoxicillin*** was used as the reference antibiotic for comparison [28, 29].

2.6. Measurement of the antioxidant activity of compounds ex vivo. To evaluate the ability of the synthesized compounds (A_{10}, A_{11}, A_{33}, A_{34}, A_{39}, A_{40}, A_{41}) to scavenge DPPH free radicals, 4 mg of each compound was dissolved in 100 mL of methanol to prepare a stock solution with a concentration of 0.1 mmol/L. Then, 3 mL of the DPPH solution was mixed with 1 mL of the compound solutions prepared at concentrations of 10%, 20%, 40%, 80%, and 100% (µg/mL). Ascorbic acid (AA), prepared at the same concentrations (10%, 20%, 40%, 80%, 100% µg/mL), was used as a positive control. The mixtures were kept in the dark for 30 minutes [30–32].

The absorbance was measured at 516 nm, and the percentage of DPPH radical scavenging activity was calculated. The scavenging ability was determined using the following equation [33, 34]:

$$\mathbf{I\% = (Abc_0 - Abc_1) / Abc_0 \times 100}$$

3. Results and discussion

The chains of compounds were created according to the following scheme 1:

3.1. Characterization of Mannich base derivatives (A_{10}-A_{14}). When studying the infrared spectra of manchine derivatives (A_{10}-A_{14}), it was observed that an absorption band

appeared in the range of (3215-3161) cm^{-1} due to the extension of the (NH) bond, an absorption band appeared in the range of (3067-3016) cm^{-1} due to the extension of the aromatic (CH) bond, an absorption band appeared in the range of (2943-2920) cm^{-1} due to the extension of the aliphatic (CH) bond, and an absorption band appeared in the range of (1605-1595) cm^{-1} due to the extension of the (C=N) bond. In addition, two absorption bands were observed in the range of 1566-1517 cm^{-1}. The absorption band in the range of (1488-1469) cm^{-1} is due to the stretching of the aromatic (C=C) bond, the absorption band in the range of (1269-1234) cm^{-1} is due to the stretching of the (C-N) bond, and the absorption band in the range of (781-756) cm^{-1} is due to the stretching of the (C-S) bond, as shown in Table 4 and Fig.s 1 and 2 [35].

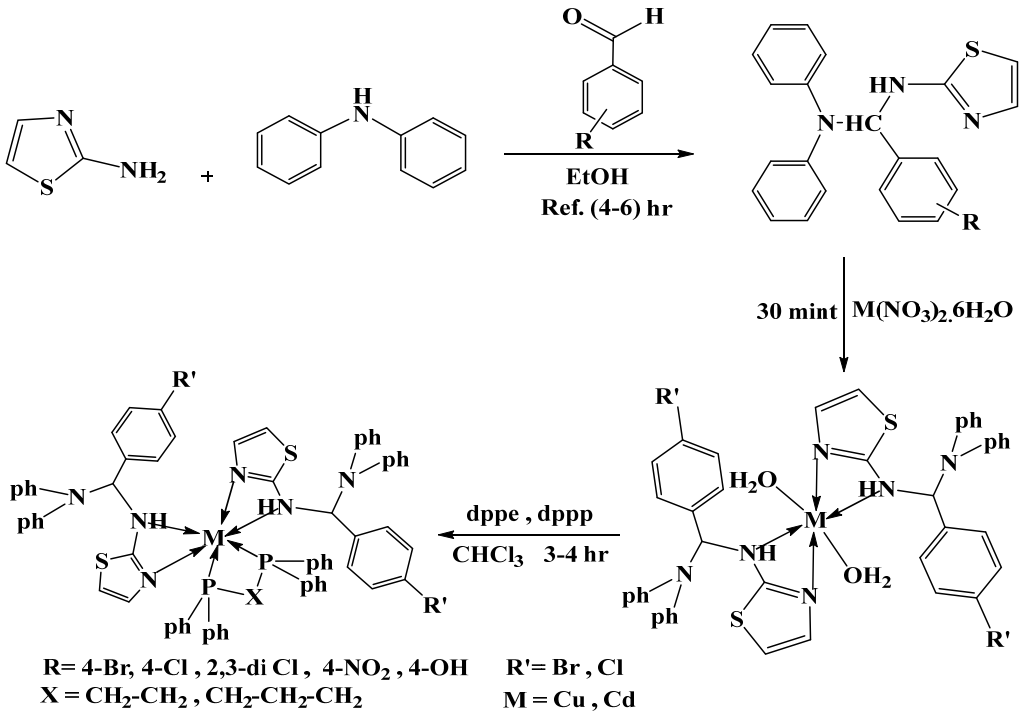

Scheme 1. Path of the ready compounds

Table 4. Infrared absorption results (cm^{-1}) for Mannich base derivatives (A_{10}-A_{14})

Comp. No.	R	IR (KBr) cm^{-1}					
		νN-H νC-H Arom.	νC-H Aliph.	νC=N	νC=C Arom.	νC-N νC-S	Others
A_{10}	4-Br	3171 3031	2941	1599	1535 1485	1269 781	ν (C-Br) 613
A_{11}	4-Cl	3191 3058	2932	1603	1540 1479	1256 762	ν (C-Cl) 751
A_{12}	2,3-di Cl	3210 3067	2943	1605	1517 1488	1234 773	ν (C-Cl) 730
A_{13}	4-NO_2	3215 3041	2929	1602	1566 1474	1251 758	ν(NO_2) *asy*. (1525) *sym*. (1337)
A_{14}	4-OH	3161 3016	2920	1595	1521 1469	1244 756	ν (OH) 3437

A single signal at the chemical shift (5.78-6.16) ppm, attributed to the proton of the (NH) group; a single signal at the chemical shift (4.92-5.05) parts per million, attributed to the proton of the (CH) group; and a multiple signal in the range (6.78-8.03) parts per million, attributed to the protons of the aromatic rings, were all observed

when examining the compounds' ^{1}H-NMR spectrum using the solvent (DMSO-d6), as shown in Table 5 and Fig.s 3 and 4.

Table 5. ^{1}H-NMR spectrum values for compounds (A_{10}-A_{14})

Comp No.	R	NH	CH	Ar-H
A_{10}	4-Br	5.78	5.04	6.81-8.03
A_{11}	4-Cl	5.99	4.95	6.92-7.90
A_{12}	2,3-Cl	6.16	4.99	7.03-7.61
A_{13}	4-NO_2	6.09	5.05	6.98-7.85
A_{14}	4-OH	5.94	4.92	6.78-7.79

When the ^{13}C-NMR spectrum of the compounds was studied using the solvent (DMSO-d6), it was found that the carbon of the (C=N) group in the thiazole ring appeared as a signal at the chemical shift (163.83) ppm, that the carbons of the aromatic ring appeared as a multiple signal at the chemical shift (122.48-141.69) ppm, that the carbon of the (CH) group appeared as a signal at the chemical shift (87.82) ppm, and that the carbon of the solvent (DMSO-d6) appeared at the chemical shift (39.34-40.59) ppm. The spectrum is displayed in Table 6 and Fig.s 5 and 6.

Table 6. ^{13}C-NMR spectrum values for compounds (A_{10}-A_{14})

Comp No.	R	C=N	CH	Ar (C=C)
A_{10}	4-Br	165.38	85.46	120.47-145.43
A_{11}	4-Cl	163.83	87.82	122.48-141.69
A_{12}	2,3-Cl	166.20	78.61	121.46-136.85
A_{13}	4-NO_2	164.48	82.15	120.23-141.22
A_{14}	4-OH	163.76	84.52	119.86-143.34

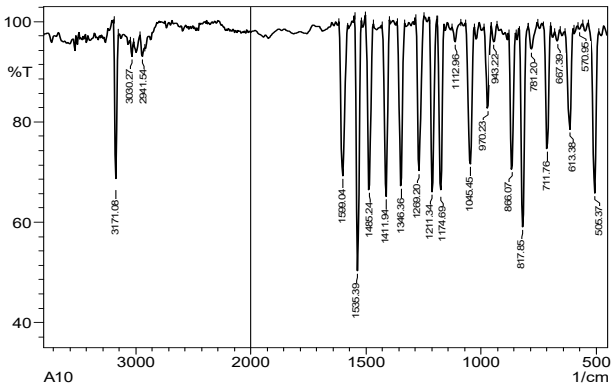

Fig. 1. Infrared spectrum of compound A_{10}

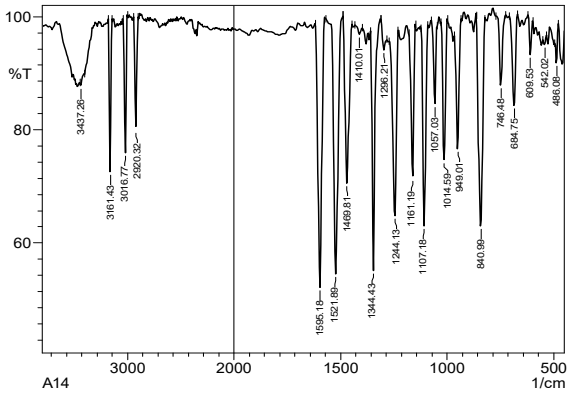

Fig. 2. Infrared spectrum of compound A_{14}

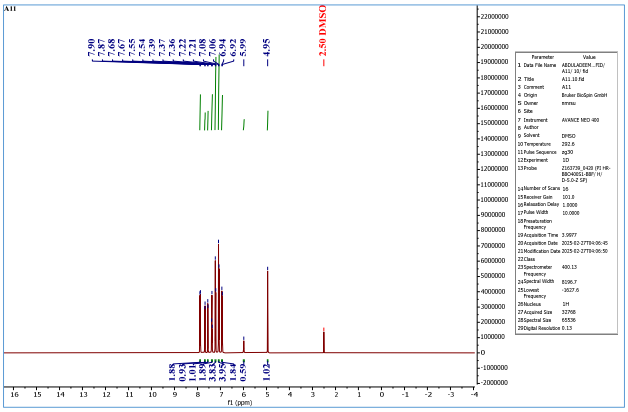

Fig. 3. ^{1}H-NMR spectrum of the compound A_{11}.

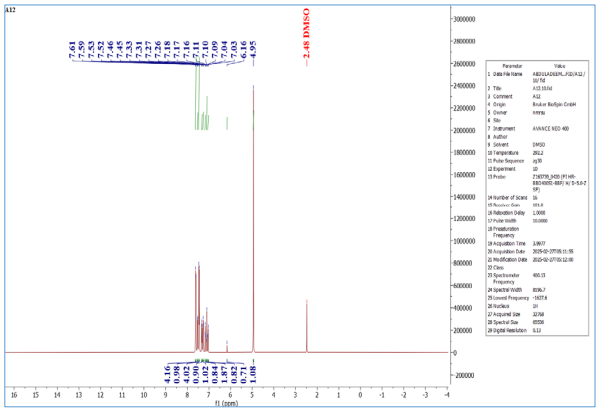

Fig. 4. ^{1}H-NMR spectrum of the compound A_{12}

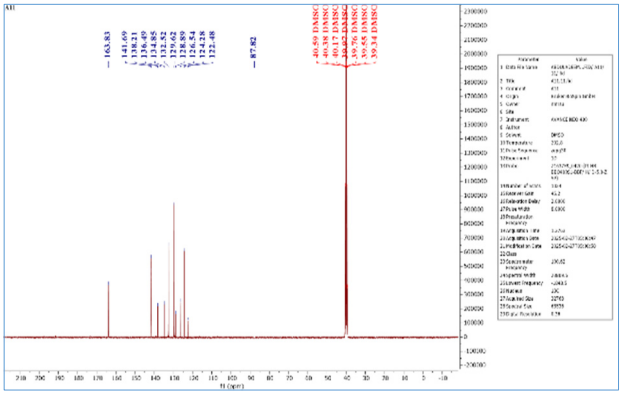

Fig. 5. ^{13}C-NMR spectrum of the compound A_{11}

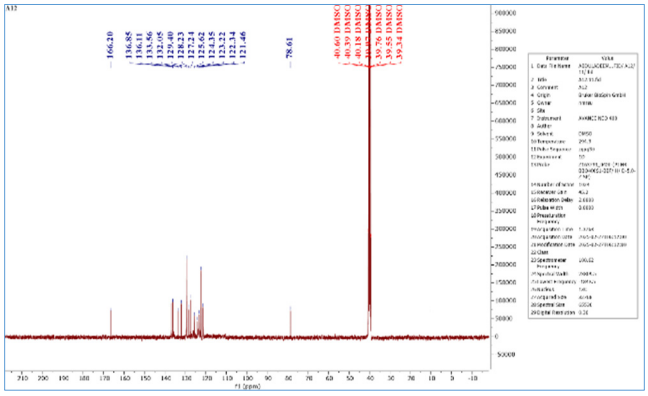

Fig. 6. ^{13}C-NMR spectrum of the compound A_{12}

3.2. Characterization of Mannich base complexes (A_{32}-A_{35}). A new absorption band appears in the range of **513–490 cm^{-1}**, corresponding to the stretching vibration of the **M–O bond**. In the infrared spectra of the Schiff base complexes (A20–A23), a noticeable decrease is observed in both the **carbonyl (C–N)** band at **1242–1236 cm^{-1}** and the **azomethine (C–S)** band at **743–723 cm^{-1}**. In addition, a new absorption band emerges in the **482–439 cm^{-1}** region, attributed to **M–N bond stretching**, while another new band appears in the **3433–3391 cm^{-1}** range, corresponding to the stretching vibration of the **O–H** group. The remaining bands in the ligands appear within similar spectral regions. A single absorption band at **3273–3235 cm^{-1}** corresponds to the stretching vibration of the **(N–H)** group. An absorption band observed at **3072–3045 cm^{-1}** is attributed to the stretching of **aromatic C–H** bonds. Two absorption bands in the ranges **2934–2920 cm^{-1}** and **2875–2852 cm^{-1}** arise from the stretching vibrations of **aliphatic C–H** bonds. Additionally, two bands at **1553–1529 cm^{-1}** and **1500–1473 cm^{-1}** are assigned to the stretching of **aromatic C=C** bonds. A distinct band at **1598–1593 cm^{-1}** corresponds to the stretching vibration of the **C=N** group. These characteristic absorptions are summarized in Table 7 and illustrated in Fig.s 7 and 8 [36].

Table 7. Infrared absorption results (cm^{-1}) for Mannich base complexes (A_{35}-A_{32})

Comp. No.	R M	IR (KBr) cm^{-1}						
		ν(OH) νN-H	νC-H Arom. νC=N	νC-H Aliph	νC=C Arom.	νC-N νC-S	νM-O νM-N	Others
A_{32}	Br Cu	3433 3255	3061 1593	2920 2852	1553 1500	1242 723	505 439	ν(C-Br)624
A_{33}	Cl Cu	3391 3254	3072 1597	2934 2868	1545 1473	1238 743	490 442	ν(C-Cl)734
A_{34}	Br Cd	3414 3235	3045 1598	2927 2875	1529 1482	1236 746	510 460	ν(C-Br)604
A_{35}	Cl Cd	3396 3273	3053 1595	2920 2862	1533 1475	1240 744	513 482	ν(C-Cl)723

3.3. Characterization of phosphine complexes of mannich bases (A_{36}-A_{43}). When examining the infrared spectra of phosphine complexes derived from Mannich bases (A_{36}–A_{43}), a characteristic band attributed to the (C–N) group was observed in the 1242–1222 cm^{-1} region. A band appearing in the 748–735 cm^{-1} range corresponded to the (C–S) group. The development of an absorption band in the 501–453 cm^{-1} region was assigned to the stretching vibration of the (M–O) bond, while a new band in the 457–425 cm^{-1} range was associated with (M–N) bond stretching. Additionally, the stretching vibration of the (P–Ph) bond produced a new absorption band in the 1439–1421 cm^{-1} region, and another band appearing at 1137–1108 cm^{-1} was attributed to (C–Ph) stretching.

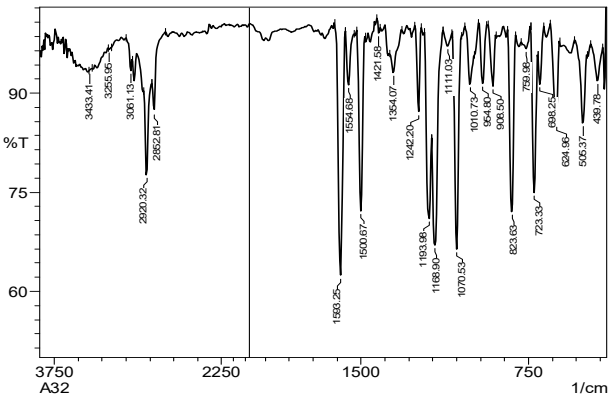

Fig. 7. FT-IR spectrum of compound A_{32}

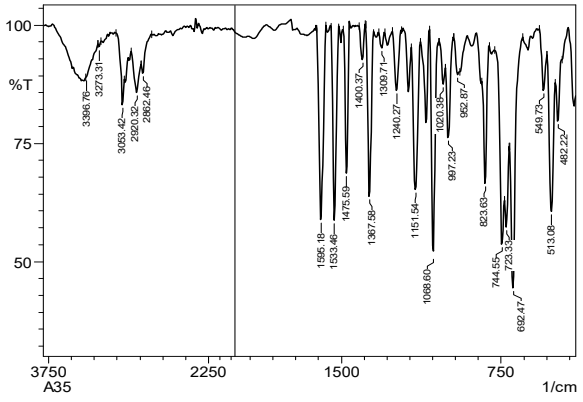

Fig. 8. FT-IR spectrum of compound A_{35}

The remaining ligand bands appeared within their expected regions. The (NH) stretching vibration generated an absorption band in the 3278–3204 cm^{-1} range, whereas aromatic (CH) stretching produced a band at 3072–3026 cm^{-1}. Two bands in the 2993–2914 cm^{-1} and 2933–2869 cm^{-1} regions corresponded to aliphatic (CH) stretching. Furthermore, the (C=N) stretching vibration gave rise to an absorption band in the 1598–1590 cm^{-1} region. Two additional bands, observed at 1531–1510 cm^{-1} and 1483–1469 cm^{-1}, were attributed to aromatic (C=C) stretching (Table 8; Fig.s 9 and 10) [37].

Table 8. Infrared absorption results (cm^{-1}) for Mannich base complexes (A_{36}-A_{43})

Comp. No.	R	M	IR (KBr) cm^{-1}							
			νN-H νC-H Arom.	νC-H Aliph.	νC=N	νC=C Arom.	νP-Ph νC-P	νC-N νC-S	νM-O νM-N	Others
A_{36}	Br	Cu dppe	3265 3059	2949 2878	1591	1524 1469	1437 1124	1235 739	467 425	ν(C-Br)616
A_{37}	Br	Cu dppp	3215 3026	2912 2870	1594	1529 1483	1430 1129	1231 741	493 432	ν(C-Cl)643
A_{38}	Cl	Cu dppe	3226 3031	2993 2933	1593	1510 1481	1432 1108	1242 746	453 437	ν(C-Cl)771
A_{39}	Cl	Cu dppp	3204 3072	2965 2883	1598	1530 1476	1427 1116	1237 745	479 438	ν(C-Cl)727
A_{40}	Br	Cd dppe	3278 3060	2924 2869	1590	1527 1470	1421 1131	1225 738	480 436	ν(C-Br)597
A_{41}	Br	Cd dppp	3242 3056	2941 2889	1596	1512 1473	1434 1137	1222 748	478 428	ν(C-Br)605
A_{42}	Cl	Cd dppe	3261 3032	2929 2873	1592	1531 1477	1424 1119	1227 735	501 457	ν(C-Cl)719
A_{43}	Cl	Cd dppp	3252 3059	2914 2875	1597	1526 1480	1439 1126	1228 744	487 440	ν(C-Cl)730

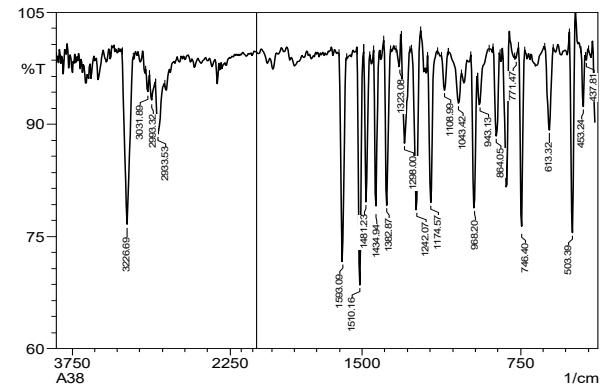

Fig. 9. FT-IR spectrum of compound A_{38}

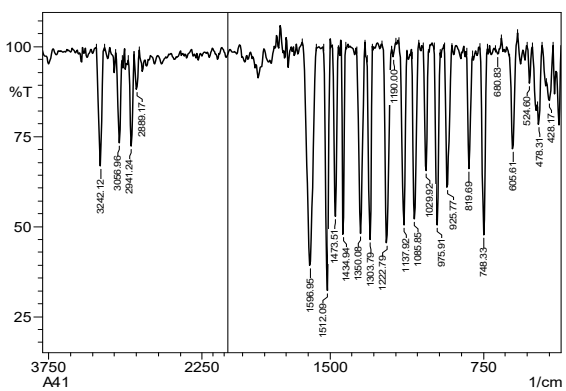

Fig. 10. FT-IR spectrum of compound A_{41}

When the ^{31}P-NMR spectra of the compounds were recorded in DMSO, a single resonance signal was observed in the chemical shift range of 32.79–38.08 ppm. This singlet corresponds to the equivalent phosphorus atoms in the complexes and confirms the presence of a single isomeric form. The data are summarized in Table 9 and illustrated in Fig.s 11–14.

Table 8. ^{31}P-NMR spectrum for Mannich base complexes (A_{36}-A_{43})

Comp. No.	R	M	^{31}P-NMR	Comp. No.	R	M	^{31}P-NMR
A_{36}	Br	Cu dppe	38.08	**A_{40}**	Br	Cd dppe	37.43
A_{37}	Br	Cu dppp	35,65	**A_{41}**	Br	Cd dppp	36.97
A_{38}	Cl	Cu dppe	32.79	**A_{42}**	Cl	Cd dppe	35.24
A_{39}	Cl	Cu dppp	34.54	**A_{43}**	Cl	Cd dppp	37.82

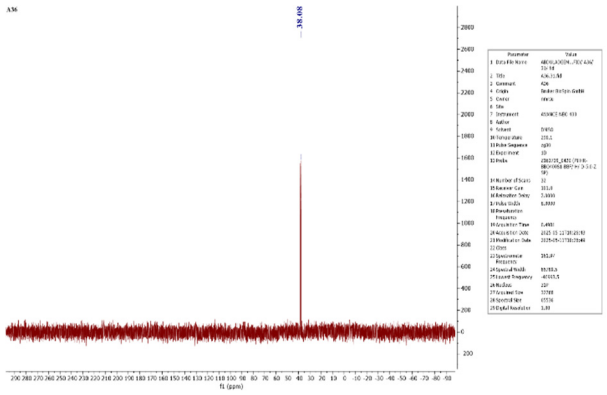

Fig.11. ^{31}P-NMR spectrum of the compound A_{36}.

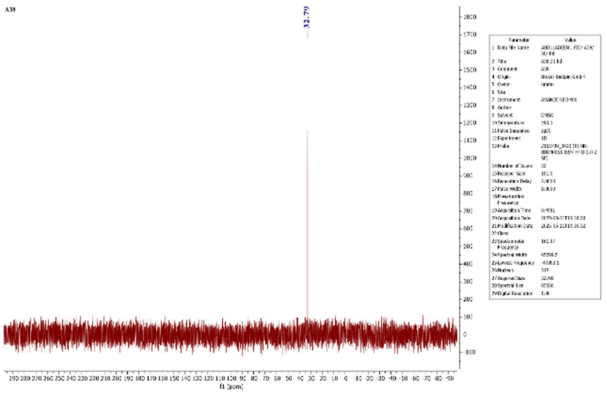

Fig.12. ^{31}P-NMR spectrum of the compound A_{38}

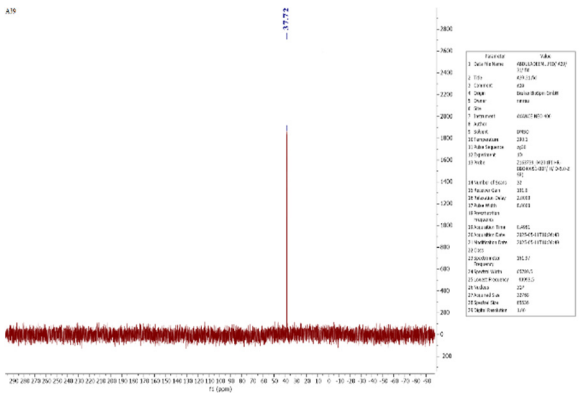

Fig. 13. ^{31}P-NMR spectrum of the compound A_{39}.

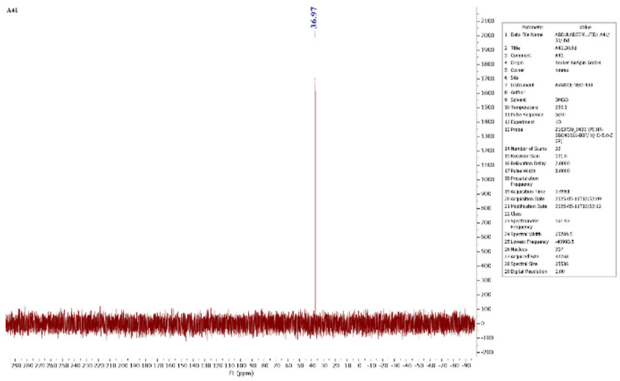

Fig. 14. ^{31}P-NMR spectrum of the compound A_{41}

3.4. Elemental Analysis (C.H.N.O.) Measurement. The manufactured compounds were subjected to elemental analysis (C.H.N.) to confirm the precision and accuracy of their structural composition. The elemental ratios that were obtained were either consistent with or very close to the calculated values, thereby validating the manufactured compounds' structures.

Table 9. Results of elemental analysis (C.H.N.O) of manufactured compounds

Comp No.	R	Complexes	Calculated				Found			
			C%	H%	N%	S%	C%	H%	N%	S%
A_{36}	Br	[Cu(A_{10})$_2$(dppe)]	62.99	4.53	6.30	4.80	63.21	4.78	6.72	4.97

A_{39}	Cl	$[Cu(A_{11})_2(dppp)]$	67.69	4.96	6.67	5.09	68.02	5.10	6.86	5.32
A_{41}	Br	$[Cd(A_{10})_2(dppp)]$	61.02	4.47	6.01	4.59	61.23	4.69	6.28	4.79
A_{42}	Cl	$[Cd(A_{11})_2(dppe)]$	64.94	4.67	6.49	4.95	65.09	4.86	6.71	5.16

3.5. Magnetic susceptibility measurements of prepared complexes [38, 39]. The magnetic susceptibility of the prepared copper and cadmium complexes was calculated at a temperature of 25°C. The diamagnetism (D) of the atoms in the organic molecules, metal ions, and inorganic radicals was corrected using Pascal's constants for the atoms forming the prepared complexes. D (g. $atom^{-1}$) = the total number of ions or atoms of the element multiplied by the value of Pascal's constant. The values of the magnetic moment (μ_{eff}) (effective magnetic moment) were calculated according to the following relationship:

$$\chi_M = \chi g * M.w$$
$$\chi_A = \chi_M - D$$

Magnetic measurements of the prepared complexes (A_{32}, A_{33}, A_{34}) showed values close to (5.12 - 3.02) B.M, which suggests that the cobalt, copper, nickel and cadmium (II) complexes are hexagonally coordinated with a highly octahedral shape, as in Table 10, which shows the magnetic susceptibility of the prepared complexes.

Table 10. Results of magnetic measurements of the prepared complexes

No.	Complexes	Gram-sensitivity $\chi g \times 10^{-6}$	Molar susceptibility $\chi M \times 10^{-6}$	Diamagnetic correction factor $D \times 10^{-6}$	Atomic susceptibility $\chi A \times 10^{-6}$	Effective magnetic moment μ_{eff} (BM)
A_{32}	$[Cu(A_{10})_2(H_2O)_2]$	12.642	10735.59	292.12	11027.71	5.126608
A_{33}	$[Cu(A_{11})_2(H_2O)_2]$	3.823	3717.179	359.44	4076.619	3.117006
A_{34}	$[Cd(A_{10})_2(H_2O)_2]$	5.462	4825.185	313.32	5138.505	3.4995

3.6. Bacterial susceptibility to prepared compounds. The biological activity of the prepared compounds (A_{12}, A_{32}, A_{34}, A_{38}, A_{40}) against two types of medically important bacteria, namely *Staphylococcus aureus (Gram-positive)* and *Escherichia coli (Gram-negative)*, was evaluated using the Well Diffusion Method to measure the diameters of inhibition at three different concentrations (100%, 50%, 25%), and compared with the activity of the standard antibiotic *Amoxicillin* [40-43]. The results showed that some of the prepared compounds possessed high inhibitory activity against the growth of the tested bacteria. Compound A_{34} recorded the highest inhibition diameter against *S. aureus*, reaching 34 mm, and a diameter of 24 mm against *E. coli*, outperforming the standard antibiotic amoxicillin. Compound A_{31} also showed outstanding activity, reaching 27 mm and 25 mm against *Gram-positive* and *Gram-negative bacteria*, respectively [44-48].

Table 11. Antibacterial activity of the synthesized compounds (inhibition zone in mm)

Comp. No	Staphylococcus Aureus (S.A)			Escherichia Coli (E.C)		
	100%	50%	25%	100%	50%	25%
A_{12}	20	18	15	12	10	9
A_{32}	23	20	17	20	18	17
A_{34}	34	31	28	24	21	19
A_{38}	21	16	12	13	10	5
A_{40}	22	17	15	15	10	5
Amoxicillin	23	17	14	18	15	12

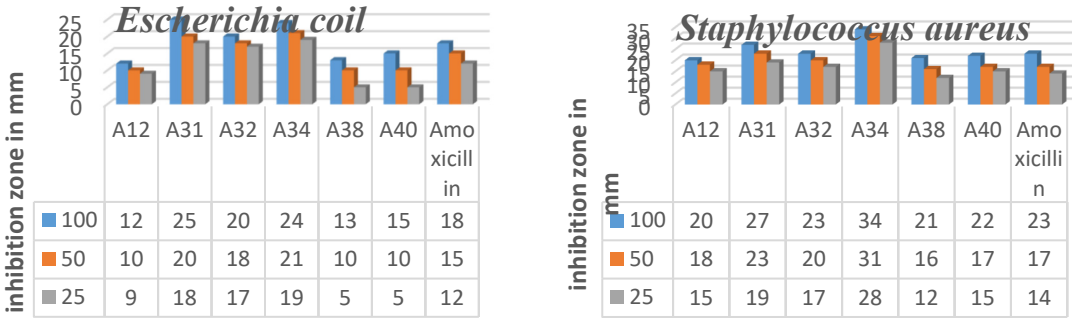

Scheme 2. Inhibitory activity for Staph. Aureus and E. Coli

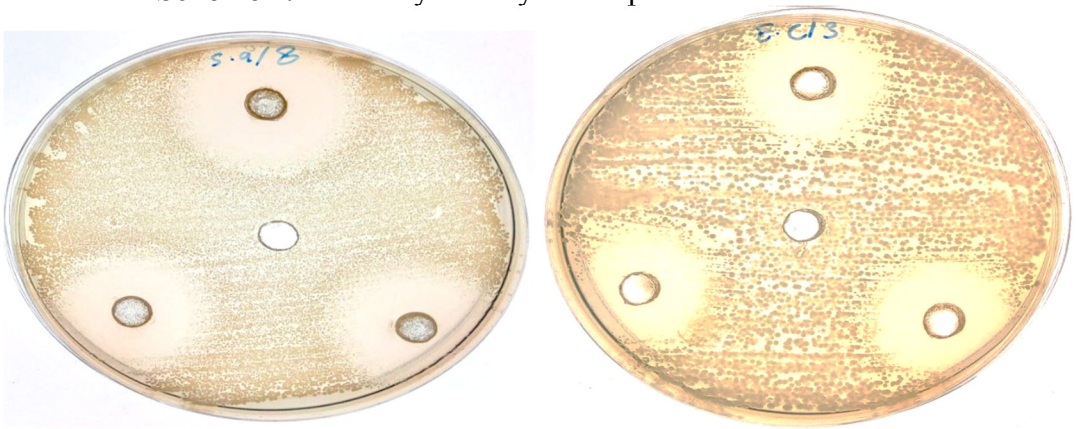

Fig. 15. Inhibitory activity of the compounds A_{31} and A_{34} against E. Coli

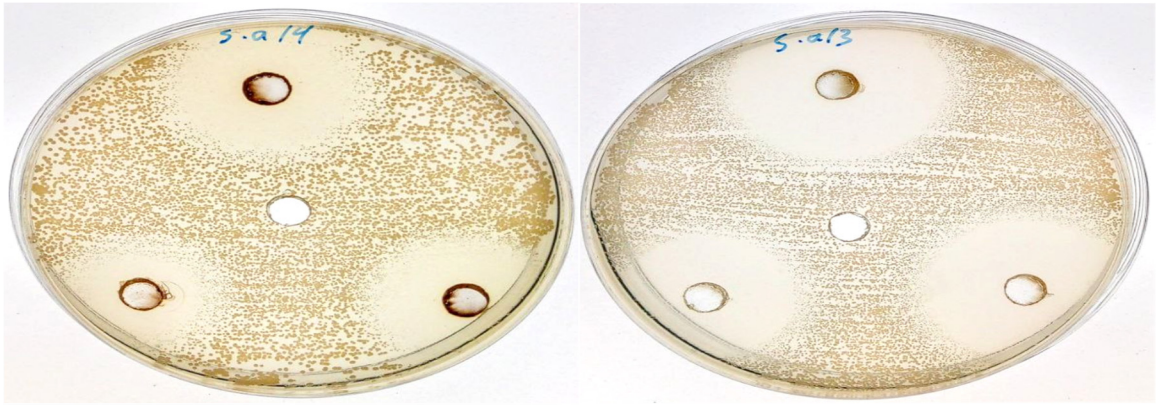

Fig. 16. Inhibitory activity of the compounds A_{31} and A_{34} against Stapfh. aureus

3.7. Measurement of antioxidant activity [49-51]. The antioxidant activity of compounds (A_{10}, A_{11}, A_{33}, A_{34}, A_{39}, A_{40}, and A_{41}) was evaluated using the DPPH assay, which is based on the discoloration of the purple DPPH* solution to yellow upon reaction with free radical scavengers. The decrease in absorbance at 517 nm was used to calculate the percentage of radical scavenging activity (%RSA), reflecting the efficiency of each compound in neutralizing DPPH* free radicals.

The results demonstrated that several compounds exhibited notable antioxidant properties, with activity increasing progressively as the concentration increased. Among the tested compounds, **A_{34}** displayed the highest activity, reaching **58.75% RSA** at the maximum concentration (100 µg/ml). This was followed by **A_{41}** and **A_{39}**, which achieved **53.75%** and **50%**, respectively, indicating strong radical-scavenging capabilities. Compounds **A_{11}** and **A_{40}** showed moderate activities of **48.75%** and **48.875%**, although their efficiencies varied at lower concentrations; notably, compound **A_{40}** exhibited a complete loss of activity at 20 and 10 µg/ml.

In contrast, **A_{10}** showed relatively weak antioxidant performance, not exceeding **41.25%**

at any concentration tested, while **A_{33}** exhibited limited but consistent activity, reaching only **31.25%**. When compared to the reference antioxidant **ascorbic acid**, which showed **62.5%** activity at the highest concentration and decreased to **35%** at the lowest concentration, compounds **A_{34}** and **A_{41}** demonstrated comparable efficiencies, suggesting their potential as alternative antioxidant agents.

A gradual increase in antioxidant activity with concentration was visually supported by the observed color change of the reaction mixtures—from dark purple to pale yellow—indicating increasing free radical inhibition. These findings highlight the promising antioxidant potential of several compounds, particularly **A_{34}** and **A_{41}**, for potential pharmaceutical or food-related applications, as presented in Table 12 and Fig. 17.

Table 12. The percentage of antioxidant activity in the form of %RSA for the prepared compounds at different concentrations

Comp. No	10%	20%	40%	80%	100%
A_{10}	10	12.5	12.5	37.5	41.25
A_{11}	25	31.25	31.25	37.5	48.75
A_{33}	18.75	25	28.75	30	31.25
A_{34}	12.5	18.75	25	56.25	58.75
A_{39}	17.5	25	27.5	37.5	50
A_{40}	0	0	37.5	43.75	48.875
A_{41}	12.5	15	25	47.5	53.75
Ascorbic acid	35	50	57.5	58.75	62.5

10 20 40 80 100# DPPH A.A 10 20 40 80 100# DPPH

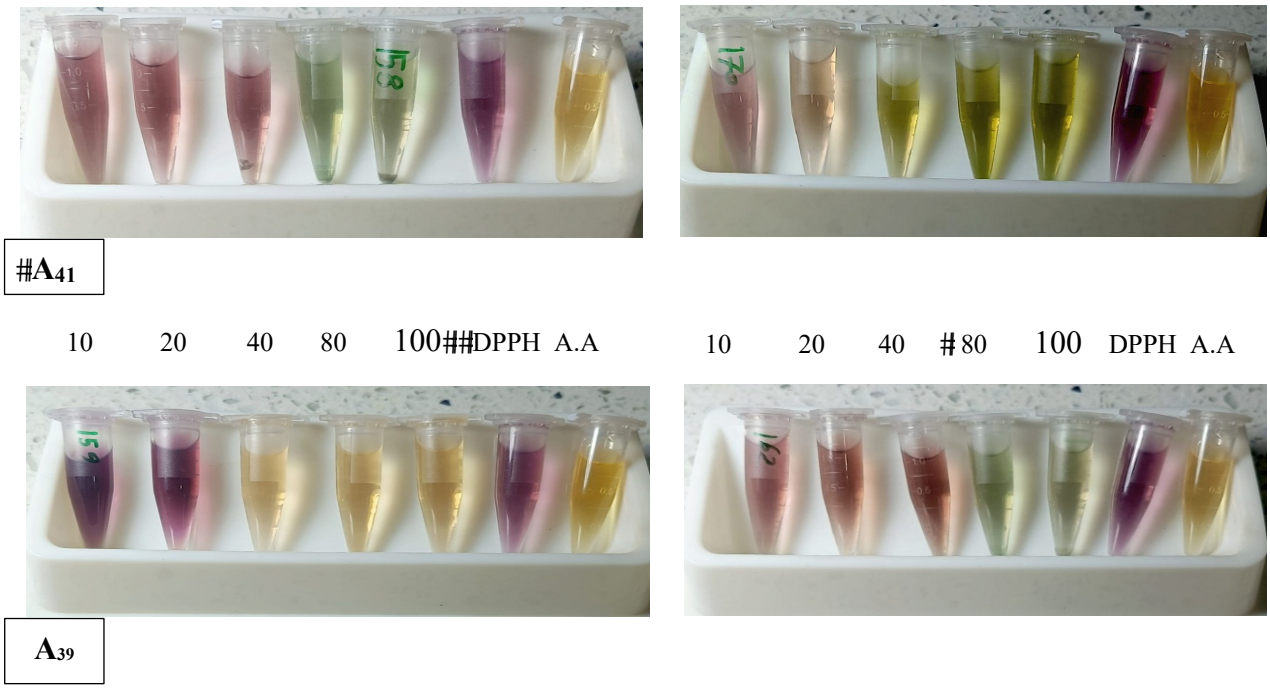

Fig. 17. Color change of compounds (A_{33}, A_{41}, A_{40}, A_{39}) with increasing concentration

4. Conclusions

The prepared compounds, including Mannich base derivatives and their corresponding metal complexes, exhibited well-defined structural characteristics supported by comprehensive spectroscopic analyses. Infrared spectroscopy, along with proton, carbon, and phosphorus NMR data, confirmed the presence of the expected functional groups and validated the proposed structures. The copper and cadmium complexes displayed spectral features characteristic of six-coordinate systems, and magnetic moment measurements further supported their octahedral geometries.

From a biological standpoint, several of the synthesized compounds demonstrated notable antibacterial activity. In particular, compound (A_{34}) showed superior performance compared with the reference antibiotic amoxicillin, indicating strong potential as a therapeutic agent. Furthermore, compounds (A_{34}) and (A_{41}) exhibited significant antioxidant activity, achieving 58.75% and 53.75% radical scavenging activity, respectively, at the highest tested concentration. Their activity levels, being comparable to that of ascorbic acid, highlight their capability as natural free-radical scavengers.

Overall, these findings underscore the promising bioactivity of the synthesized Mannich derivatives and their metal complexes. The results provide a solid foundation for further investigations aimed at evaluating their pharmacological potential, toxicological profiles, and broader biological applications across different systems.

References

1. Chen G., Yuan W., Su H., Zhang J., Gu X., Bai Y., Jeje A. Methanol enhanced catalytic viscosity-reduction of heavy oil by transition metal-Mannich base complex under low temperature. *Russian Journal of Applied Chemistry*, 2016, **Vol. 89**, p. 1853-1860. DOI: 10.1134/S1070427216110173
2. Abu-Dief A.M., Mohamed I.M. A review on versatile applications of transition metal complexes incorporating Schiff bases. *Beni-suef university journal of basic and applied sciences*, 2015, **Vol. 2**, p. 119-133. DOI: 10.1016/j.bjbas.2015.05.004
3. Al-Jeboori M.J., Al-Dujaili A.H., Al-Janabi A.E. Coordination of carbonyl oxygen in the complexes of polymeric N-crotonyl-2-hydroxyphenylazomethine. *Transition metal chemistry*, 2009, **Vol. 34**, p. 109-113. DOI: 10.1007/s11243-008-9165-9
4. Bhirud R.G., Srivastava T.S. Superoxide dismutase activity of Cu (II) 2 (aspirinate) 4 and its adducts with nitrogen and oxygen donors. *Inorganica Chimica Acta*, 1990, **Vol. 1**, p. 121-125. DOI: 10.1016/S0020-1693(00)91063-6
5. Ramadevi P., Singh R., Jana S.S., Devkar R., Chakraborty D. Ruthenium complexes of ferrocene mannich bases: DNA/BSA interactions and cytotoxicity against A549 cell line. *Journal of Photochemistry and Photobiology A: Chemistry*, 2015, **Vol. 305**, p. 1-10. DOI: 10.1016/j.jphotochem.2015.02.010
6. Berk B., Ertaş M., Biltekin S.N. Synthesis, antimicrobial activity studies and molecular property predictions of schiff bases derived from ortho-vanillin. *ACTA Pharmaceutica Sciencia*, 2017, **Vol. 55(1)**, p. 83-96. DOI: 10.23893/1307-2080.APS.0556
7. Karthikeyan N.S., Sathiyanarayanan K.I., Aravindan P.G. Ammonium Acetate: An Efficient Reagent for the One-pot Synthesis of 5-Aryl-7, 8, 13, 14-tetrahydrodibenzo [a, i] phenanthridines, 2, 4-Diaryl-6, 7-benzo-3-azabicyclo [3.3. 1] nonan-9-ones and α, α'-Bis (substituted benzylidene) cycloalkanones. *Bulletin of the Korean Chemical Society*, 2009, **Vol. 30(11)**, p. 2555-2558. DOI: 10.5012/bkcs.2009.30.11.2555
8. Memon S., Bhatti A.A., Ocak Ü., Ocak M. Cu^{2+} selective chromogenic behavior of calix [4] arene derivative. *Polycyclic Aromatic Compounds*, 2016, **Vol. 36(4)**, p. 395-409. DOI: 10.1080/10406638.2014.994070
9. Jia P., Hu L., Shang Q., Wang R., Zhang M., Zhou Y. Self-plasticization of PVC materials via chemical modification of mannich base of cardanol butyl ether. *ACS Sustainable Chemistry & Engineering*, 2017, **Vol. 5(8)**, p. 6665-6673. DOI: 10.1021/acssuschemeng.7b00900
10. Liaqat M., Mahmud T., Imran M., Iqbal M., Muddassar M., Ahmad T., Mitu L. Synthesis, Characterization and Biological Study of a New Mannich Base, 2-[(4-fluorophenyl)(phenylamino) methyl] cyclopentanone (FPC) and its Transition Metal Complexes with Cu (II), Ni (II), Co (II), Fe (II) and Zn (II). *Rev. Chim. (Bucharest)*, 2017, **Vol. 68(11)**, p. 25560-25565. DOI: 10.37358/RC.17.11.5928
11. Muruganandam L., Krishnakumar K., Balasubramanian K. Synthesis, Characterization and Antimicrobial Studies

of a Few Mn II, Fe II, Zn II, Cd II and Hg II Complexes Derived from N-[Morpholino (phenyl) methyl] acetamide as New Mannich Base Ligand. *Che. Sci. Rev.*, 2012, **Vol. 1(2)**, p. 78-83.
12. Sundaravadivel E., Reddy G.R., Manoj D., Rajendran S., Kandaswamy M., Janakiraman M. DNA binding and cleavage studies of copper (II) complex containing N_2O_2 Schiff base ligand. *Inorganica Chimica Acta*, 2018, **Vol. 482**, p. 170-178. DOI: 10.1016/j.ica.2018.06.002
13. Chaisuwan T., Komalwanich T., Luangsukrerk S., Wongkasemjit S. Removal of heavy metals from model wastewater by using polybenzoxazine aerogel. *Desalination*, 2010, **Vol. 256(1-3)**, p. 108-114. DOI: 10.1016/j.desal.2010.02.005
14. Segnini D., Curran C., Quagliano J.V. Infrared absorption studies of inorganic co-ordination complexes—XXIII: Studies of some metal-alanine complexes. *Spectrochimica Acta*, 1960, **Vol. 16(5)**, p. 540-546. DOI: 10.1016/0371-1951(60)80010-0
15. Supriya S., Raghavan A., Vijayaraghavan V.R., Chinnakali K., Fun H.K., Subramanian J. Mannich aminomethylation reactions of a series of bis (α-amino acidato) metal (II) complexes with formaldehyde and diethylmalonate: Crystal structure of (5, 5-dicarboxyethyl-3, 7-diazanonanedioato) copper (II) monohydrate. *Polyhedron*, 2007, **Vol. 26(13)**, p. 3217-3226. DOI: 10.1016/j.poly.2007.02.017
16. Belinelo V.J., Reis G.T., Stefani G.M., Ferreira-Alves D.L., Piló-Veloso D. Synthesis of 6a, 7b-dihydroxyvouacapan-17b-oic acid derivatives. Part IV: mannich base derivatives and its activities on the electrically stimulated Guinea-pig ileum preparation. *Journal of the Brazilian Chemical Society*, 2002, **Vol. 13(6)**, p. 830-837. DOI: 10.1590/S0103-50532002000600016
17. Latypova D.R., Badamshin A.G., Lobov A.N., Dokichev V.A. Reaction of ethyl acetoacetate with formaldehyde and primary amines. *Russian Journal of Organic Chemistry*, 2013, **Vol. 49**, p. 843-848. DOI: 10.1134/S1070428013060079
18. Quiroga D., Coy-Barrera E. Synthesis of Antifungal Heterocycle-Containing Mannich Bases: A Comprehensive Review. *Organics*, 2023, **Vol. 4(4),** p. 503-523. DOI: 10.3390/org4040035
19. Hameed M.A., Al-Jeboori M.J. Synthesis, spectral characterisation, DFT calculations, biological evaluation and molecular docking analysis of new Mannich compounds derived from cyclopentanone. *Journal of Molecular Structure*, 2025, **Vol. 1322(4)**, 140619. DOI: 10.1016/j.molstruc.2024.140619
20. Ramasamy M., Velayutham G., Pitchaipillai R. A Novel Mannich Based Metal II Complexes: Synthesis and Characterization of Magnetic, Conductivity and Antimicrobial Properties. *Eurasian Journal of Chemistry*, 2025, **Vol. 1(117)**, p. 60-75. DOI: 10.31489/2959-0663/1-25-5
21. Khalaf A.A., Shihab A.S. Synthesis, Characterization, Study of Biological Activity, and Molecular Docking of Some Mannich Bases and their Coordination with Cadmium and Cobalt. In *Macromolecular Symposia*. 2025, **Vol. 414(1)**, 2400212. DOI: 10.1002/masy.202400212
22. Aziz N.M., Irzoqi A.A. Synthesis, characterization, and biological evaluation of zinc (II) complexes with benzohydrazide derivative and phosphine ligands. *Bulletin of the Chemical Society of Ethiopia*, 2025, **Vol. 2**, p. 313-326. DOI: 10.4314/bcse.v39i2.10
23. Shubham Naina V.R., Roesky P.W. Luminescent tetranuclear copper (I) and gold (I) heterobimetallic complexes: A phosphine acetylide amidinate orthogonal ligand framework for selective complexation. *Chemistry–A European Journal*, 2024, **Vol. 30(42)**, e202401696. DOI: 10.1002/chem.202401696
24. Al-Badrani H., Ezzat N.S., Al-Jawaheri Y.S. Synthesis of oxazepino compound via electrophilic cyclization and evaluation of their biological activity. *Chemical Problems*, 2025, **Vol.** (3), p. 343-355. DOI: 10.32737/2221-8688-2025-3-343-355
25. Murad Z.A., Hamad A.S. Preparation and diagnosis of new derivatives of the tetrazole ring derived from 2-bromoisophthaladehyde and evaluation of their biological effectiveness. *Chemical Problems*, 2025,

Vol. **23(1)**, p. 116-124. DOI: 10.32737/2221-8688-2025-1-116-124
26. Najm R.S., AL-Rasheed A.A., Mohammed A.S., Graba B., Saleh M.J. Synthesis, Chemical Characterization and Biological Activity Evaluation of Lamb Meat-Derived Nanocomposite. *Advanced Journal of Chemistry, Section A*, 2025, **Vol. 12**, p. 1890-1903. DOI: 10.48309/AJCA.2025.524268.1849
27. Khalil S.L., Saleem N.H. Synthesis and characterization of five-membered heterocyclic compounds of tetrazole derivatives and their biological activity. *Chemical Problems*, 2025, **Vol**. **23(3)**, p. 365-374. DOI: 10.32737/2221-8688-2025-3-365-374
28. Hassan B.A., Mekky A.H. Synthesis, characterization and antibacterial activity of [1, 2, 4] triazolo [4, 3-b][1, 2, 4, 5] tetrazine derivatives. *Chemical Problems*, 2025, **Vol**. **23(1)**, p. 78-94. DOI: 10.32737/2221-8688-2025-1-78-94
29. Wadee S.A., Majeed H.M., Najm R.S. Evaluations of Antibacterial Efficiency of $NiFe_2O_4$ Nanoparticles Alone and in Combination with Some Antibiotics Against Multidrug Resistant Proteus Mirabilis. *Teikyo Medical Journal*, 2021, **Vol**. **44(6)**, p. 3127-3135.
30. Cornea A.C., Marc G., Ionuț I., Moldovan C., Stana A., Oniga S.D., Pirnau A., Vlase L., Oniga I., Oniga O. Synthesis, characterization, and antioxidant activity Evaluation of new N-Methyl substituted Thiazole-Derived polyphenolic compounds. *Molecules*, 2025, **Vol**. **30(6)**, 1345. DOI: 10.3390/molecules30061345
31. Vlocskó R.B., Mastyugin M., Török B., Török M. Correlation of physicochemical properties with antioxidant activity in phenol and thiophenol analogues. *Scientific Reports*, 2025, **Vol**. **15**, 73. DOI: 10.1038/s41598-024-83982-4
32. Baldelli A., Aguilera J.M. Size reduction and particle size influence the quantification of phenolic-type compounds and antioxidant activity in plant food matrices. *Trends in Food Science & Technology*, 2025, **Vol**. **162**, 105081. DOI: 10.1016/j.tifs.2025.105081
33. Shakuri F., Eghlima G., Behboudi H., Babashpour-Asl M. Phytochemical variation, phenolic compounds and antioxidant activity of wild populations of Iranian oak. *Scientific Reports*, 2025, **Vol. 15**, 6534. DOI: 10.1038/s41598-025-90991-4
34. Linares-Castañeda A., Jiménez-Martínez C., Cedillo-Olivos A.E., Cruz-Narváez Y., Corzo-Ríos L.J. Effects of hydrogen peroxide (H_2O_2) elicitation on protein content and digestibility, phenolic compounds, and antioxidant activity in sprouted chickpeas (Cicer arietinum L.). *Applied Food Research*, 2025, **Vol**. **5(1)**, 100785. DOI: 10.1016/j.afres.2025.100785
35. Abdula A.M., Qarah A.F., Alatawi K., Qurban J., Abualnaja M.M., Katuah H.A., El-Metwaly N.M. Design, synthesis, and molecular docking of new phenothiazine incorporated N-Mannich bases as promising antimicrobial agents. *Heliyon*, 2024, **Vol**. **10(7)**, e28573. DOI: 10.1016/j.heliyon.2024.e28573
36. Manhee T.Q., Alabdali A.J. Synthesis, characterization and anticancer activity of Ni (II), Cu (II), Pd (II) and Au (III) complexes derived from novel Mannich base. *Vietnam Journal of Chemistry*, 2024, **Vol**. **62(2)**, p. 201-210. DOI: 10.1002/vjch.202300141
37. Saleh M.M. Al-Nassiry A.L., Saleh J.N., Saleh M.J. Preparation and Diagnosis of New Complexes for Hg (II) With 4-Amino Acetanilide And (Dppp) As A Ligand and Study Of The Bacterial Efficacy And Molecular Docking Of The Prepared Complexes. *Central Asian Journal of Theoretical and Applied Science*, 2024, **Vol**. **5(4)**, 364-373.
38. Li J.X., Xiong L.Y., Fu L.L., Bo W.B., Du Z.X., Feng X. Structural diversity of Mn (II) and Cu (II) complexes based on 2-carboxyphenoxyacetate linker: Syntheses, conformation comparison and magnetic properties. *Journal of Solid State Chemistry*, 2022, **Vol**. **305**, 122636. DOI: 10.1016/j.jssc.2021.122636
39. Abdou A., Mostafa H.M., Abdel-Mawgoud A.M.M. Seven metal-based bi-dentate NO azocoumarine complexes: Synthesis, physicochemical properties, DFT calculations, drug-likeness, in vitro antimicrobial screening and molecular

docking analysis. *Inorganica Chimica Acta*, 2022, **Vol**. **539**, 121043. DOI: 10.1016/j.ica.2022.121043
40. Abdullah S.H., Salih M.M., Al-Badrany A. Synthesis, Characterization and Antibacterial Evaluation of Novel Thiazolidine Derivatives. *Journal of Angiotherapy*, 2024, **Vol**. **1(3)**, p. 1-9.
41. Alrashidy A.A.M., Hashem O.A., ALBadrany K.A.A. Spectrophotometric Determination of Vitamin C Using Indirect Oxidation with a New Organic Dye. *Journal of Angiotherapy*, 2024, **Vol**. **8(2)**, p. 1-7. DOI: 10.25163/angiotherapy.829499
42. Al-Joboury N.A., Al-Badrany K.A., Hamed A.S., Aljoboury W.M. Synthesis of some new thiazepine compounds derived from chalcones and evaluation there biochemical and biological activity. *Biochemical & Cellular Archives*, 2019, **Vol**. **19(2),** p. 4545-4554. DOI:1 0.35124/bca.2019.19.2.4545
43. Saleh R.H., Rashid W.M., Dalaf A.H., Al-Badrany K.A., Mohammed O.A. Synthesis of some new thiazolidinone compounds derived from schiff bases compounds and evaluation of their laser and biological efficacy. *Ann Trop & Public Health*, 2020, **Vol**. **23(7)**, p. 455-469. DOI: 10.36295/ASRO.2020.23728
44. Aftan M.M., Jabbar M.Q., Dalaf A.H., Salih H.K. Application of biological activity of oxazepine and 2-azetidinone compounds and study of their liquid crystalline behavior. *Materials Today: Proceedings*, 2021, **Vol. 43(2)**, p. 2040-2050. DOI: 10.1016/j.matpr.2020.11.838
45. Ahmed S.E., Ahmed Z.A.G., Mustafa G.S., Saleh M.J., Saleh J.N. Preparation and Characterization of New Azetidine Rings and Evaluation of Their Biological Activity. *Advanced Journal of Chemistry, Section A*, 2026, **Vol. 9(1)**, p. 146-154. DOI: 10.48309/AJCA.2026.538779.1898.
46. Hassan Z.Q.M., Abdulkarim M.G. Synthesis, characterization, and biological activity evaluation of chalcones and pyrazole derivatives derived from indole. *AL-Yarmouk Journal*, 2023, **Vol. 21(2)**, p. 42-52.
47. Abdullah S.H., Khairallah B.A., Al-Badrany K.A. Preparation and characterization of some azetidine-2-one derivatives derived from benzothiazole-2-ol and evaluation of their biological activity. *Indian Journal of Heterocyclic Chemistry*, 2025, **Vol**. **35(1)**, 37. DOI: 10.59467/IJHC.2025.35.37
48. Al Rashidy A.A.M., Al Badrany K.A., Al Garagoly G.M. Spectrophotometric determination of sulphamethoxazole drug by new pyrazoline derived from 2, 4-dinitro phenyl hydrazine. *In Materials Science Forum,* 2020, **Vol. 1002**, p. 350-359. DOI: 10.4028/www.scientific.net/MSF.1002.350
49. Thi Pham T.N., Nguyen T.T., Le Thi Nguyen T., Nguyen Tran A.M., Nguyen T.N., Tong D. T., Tien Le D. Antioxidant and Anti-Inflammatory Activities of Phytochemicals from Ruellia tuberosa. *Journal of Chemistry*, 2022, **Vol**. **2022**, 464464.14p. DOI: 10.1155/2022/4644641
50. Martínez-Cabanas M., López-García M., Rodríguez-Barro P., Vilariño T., Lodeiro P., Herrero R., Barriada J.L., Sastre de Vicente M.E. Antioxidant capacity assessment of plant extracts for green synthesis of nanoparticles. *Nanomaterials*, 2021, **Vol**. **11(7)**, 1679. DOI: 10.3390/nano11071679
51. Sayed A.E., Hafez A., Ateya A., Darwish A., Tahoun A. Single nucleotide polymorphisms, gene expression and evaluation of immunological, antioxidant, and pathological parameters associated with bacterial pneumonia in Barki sheep. *Irish Veterinary Journal*, 2025, **Vol**. **78,** 11. DOI: 10.1186/s13620-025-00296-1